doi:10.4149/neo_2021_210226N250

microRNA-10a-5p overexpression suppresses malignancy of colon cancer by regulating human liver cancer fibroblasts

Xuan ZHENG[1,#], Jing-Wu LI[2,#], Yan-Kun LIU[2,#], Yi-Fu MA[3], Jian-Hui GAN[4], Su-Gui HAN[1], Jian WANG[5], Zhao-Yuan WAN[2], Jun ZHANG[2], Yan LIU[2,6], Yu-Feng LI[2,*], Guang-Ling ZHANG[7,*]

[1]Nuclear Medicine Clinical Laboratory, Tangshan People's Hospital, Tangshan, Hebei, China; [2]The Cancer Institute, Tangshan People's Hospital, Tangshan, Hebei, China; [3]Department of Radiology, Second Affiliated Hospital of Soochow University, Suzhou, Jiangsu, China; [4]Department of Anesthesiology, Tangshan People's Hospital, Tangshan, Hebei, China; [5]Department of Gastrointestinal Surgery, Tangshan People's Hospital, Tangshan, Hebei, China; [6]College of Life Sciences, North China University of Science and Technology, Tangshan, Hebei, China; [7]School of Clinical Medicine, North China University of Science and Technology, Tangshan, Hebei, China

**Correspondence: fengfly01@163.com; zhanggl@ncst.edu.cn*
[#]Contributed equally to this work.

Received February 26, 2021 / Accepted June 10, 2021

The crosstalk between tumor and stroma plays a critical role in cancer metastasis. However, the function of miR-10a-5p on liver fibroblasts in the metastatic microenvironment of colon cancer (CC) and the effect of activated fibroblasts on CC cells are still unclear. In our study, miR-10a-5p overexpression inhibited the proliferation, migration, and IL-6/IL-8 level of LX-2 cells and human liver cancer fibroblasts (HLCFs). Moreover, miR-10a-5p had lower expression in HLCFs than in human liver normal fibroblasts (HLNFs). The conditioned medium (CM) from LX-2 cells with miR-10a-5p overexpression or HLNFs could inhibit the invasion, migration, and stemness of CC SW480 cells, whereas HLCFs CM could promote these malignant phenotypes of SW480 cells. The present study illustrates the effect of miR-10a-5p on the liver fibroblasts and the altered liver fibroblasts in the microenvironment on CC cells induced by miR-10a-5p, which may aid the understanding of the mechanisms underlying CC liver metastasis.

Key words: colon cancer liver metastasis, fibroblasts, miR-10a-5p, tumor microenvironment

Colon cancer (CC) is one of the most common types of malignant tumor worldwide [1]. In China, the rates of morbidity and mortality of CC are 14.2/100,000 and 7.4/100,000, respectively [2]. Invasion and metastasis are the main causes of colon cancer death [3]. Metastases spread to all parts through hematogenous or lymphangitic routes, such as lymph nodes, liver, lung, peritoneum, brain, and bone [4]. In distant organ metastasis, the liver is the most frequent target organ of CC metastases [5]. The prognosis of patients with distant metastasis, especially for patients with liver metastasis, is extremely poor [6]. More studies on the molecular mechanisms governing the CC metastasis need to be performed.

Tumor metastasis is a complex and multistep process [7], including tumor cell adhesion, cell invasion, extracellular matrix remodeling, angiogenesis, genesis of lymphatic vessels, and immune system [8]. Each of these processes is affected by nonmalignant cells of the tumor microenvironment (TME) [9]. TME not only includes tumor cells themselves, but also includes extracellular matrix (ECM), immune cells, soluble molecules, and stromal cells, such as cancer-associated fibroblasts (CAFs), etc. [10]. The 'activated' fibroblasts within the tumor stroma have been termed CAFs, and they can promote tumor development and metastasis by secreting a variety of growth factors, cytokines, chemokines, and degrading extracellular matrix proteins [11, 12]. For example, CAFs co-cultured with oral squamous cell carcinoma (OSCC) enhanced the migration and invasion ability of OSCC by secreting C-C motif chemokine ligand 7 (CCL7) [13]. Furthermore, miR-200s by targeting friend leukemia virus integration 1 (FLI-1) and transcription factors 12 (TCF12) in CAFs promoted ECM remodeling, which could promote the invasion and metastasis of breast cancer cells both *in vitro* and *in vivo* [14]. However, the interactions between CC cells and fibroblasts that affect the liver metastasis of colon cancer are largely unclear.

MicroRNAs (miRNAs) are essential biological functional regulators of cell proliferation, apoptosis, and differentiation by regulating the target gene expression by partial or complete base pairing [15–17]. miRNAs also play impor-

tant role in the occurrence and metastasis of inflammatory-related tumors [18]. Recently, studies indicate that miRNAs can regulate the activity of CAFs by targeting different signal pathways and metabolic matrices, thus participating in the complex signal network between tumor cells and CAFs [19, 20]. For example, miR-335 upregulation in CAFs inhibits PTEN expression, thus advances migration and invasion of gastric cancer cells [19]. In addition, downregulation of miR-1 in lung cancer CAFs promotes the secretion of stromal cell-derived factor 1 (SDF1), which promotes lung cancer cell proliferation and cisplatin resistance through nuclear factor kappa-B (NF-κB) and B-cell lymphoma XL (Bcl-XL) signaling pathways [20].

Our previous study demonstrated that exosomal-miR-10a derived from colon cancer cells suppresses proliferation, migration, and cytokines expression of human lung normal fibroblasts [21], which partly inhibited the CC primary cell metastases. However, the role of miR-10a-5p in liver fibroblasts activation and the influence of altered fibroblasts on the metastatic potential of CC cells, remains unclear. In the present study, we used LX-2 cells (one of two fibroblasts in the liver) and human liver cancer fibroblasts (HLCFs, established from colon cancer patient with liver metastasis) to study the function of miR-10a-5p on activation of fibroblasts in the liver and the crosstalk between liver fibroblasts and CC cell line SW480.

Patients and methods

Primary cells preparation. The tissues were obtained from a 54-year-old female patient who was pathologically diagnosed with colon cancer with liver metastasis in October 2018. All procedures were conducted with the approval of the Ethical Committee of Tangshan People's Hospital (Approval No.: RMYY-LLKS-2020-002). The patient's informed consent was obtained before the start of the study. Firstly, fresh normal liver tissue (>5.0 cm away from the tumor) and liver metastatic cancer tissue of a patient with CC were collected and rapidly placed into Dulbecco's modified Eagle's F12 medium (DMEM/F12) (Gibco, Carlsbad, CA, USA) supplemented with 10% fetal bovine serum (FBS) (Gibco, Carlsbad, CA, USA), 100 U/ml penicillin, and 0.1 mg/ml streptomycin. Within 30 min, the sample was washed three times with PBS and cut into approximately 1.0 mm^3 fragments. The small tissue fragments were then collected into a cell culture flask filled with DMEM/F12 supplemented with 10 ng/ml epidermal growth factor (EGF) (PeproTech, Rocky Hill, NJ, USA), 20% FBS, 100 U/ml penicillin, and 0.1 mg/ml streptomycin, and cultured at 37 °C in a humidified incubator with 5% CO_2. During the process of cell culture, DMEM/F12 was replaced every 2–3 days until cell confluence reached 80%. For the present study, the 3–8 passages of the two kinds of cells were used.

Cell culture. The human hepatic stellate cell line LX-2 was donated by Shijiazhuang Fifth Hospital and cultured in Dulbecco's modified Eagle's medium (DMEM) (Gibco, Carlsbad, CA, USA) containing 10% FBS, 100 U/ml penicillin, and 0.1 mg/ml streptomycin. The human CC cell line SW480 was donated by Tianjin Medical University and cultured in Minimal Essential Medium (MEM)-α (Gibco, Carlsbad, CA, USA) supplemented with 10% FBS, 100 U/ml penicillin, and 0.1 mg/ml streptomycin. The 0.25% trypsin-EDTA (Gibco, Carlsbad, CA, USA) was used to digest parietal cells. Cultures were incubated in a cell incubator in atmosphere containing 5% CO_2 at 37 °C.

Cell immunofluorescence assay. The third generation of human liver normal fibroblasts (HLNFs) and HLCFs were seeded into 6-well plates (1×10^5 cells/well) and incubated in a 37 °C incubator with 5% CO_2. After 48 h, cells were washed with 1× PBS, then fixed with 4% paraformaldehyde in PBS for 30 min at 37 °C, and permeabilized for 10 min 0.2% Triton X-100 in PBS (Sigma, St. Louis, MO, USA). Next, the cells were blocked by 5% (w/v) bovine serum albumin (BSA) (Amresco, Solon, OH, USA) to suppress the nonspecific reaction for 60 min. Cells were then incubated with primary anti-Cytokeratin 18 antibody (anti-CK-18) (Abcam, Cambridge, MA, USA, ab32118, 1:300), primary anti-alpha smooth muscle Actin antibody (anti-α-SMA) (Saierbio, Tianjin, China, SRP05217, 1:300), and primary anti-Fibroblast-specific protein 1 antibody (anti-FSP-1) (Abcam, Cambridge, MA, USA, ab197896, 1:300), overnight at 4 °C. Then, cells were washed three times with 1× PBS and incubated with the Alexa Fluor-555 conjugated goat anti-rabbit secondary antibodies (ThermoFisher Scientific, Waltham, MA, USA, A21430, 1:500) diluted in a blocking buffer for 45 min in the dark. Finally, DAPI (Vector Laboratories, Burlingame, CA, USA) was used for nuclei staining at room temperature for 5 min. Cells were observed under an IX71 fluorescence microscope (Olympus, Tokyo, Japan).

Flow cytometry assay. For identifying the purity of primary cells, the third generation of HLNFs and HLCFs 1×10^6 cells were harvested to detect CK-18 and α-SMA. Cells were blocked with blocking buffer (5% BSA in PBS) after one washing, fixed with 2% paraformaldehyde, and incubated at room temperature for 10 min. Then, cells were washed three times and permeabilized by permeabilization solution (0.1% Triton X-100 in PBS) for 10 min. Next, cells were washed three times, incubated in a blocking buffer for 30 min at room temperature, and treated with the anti-CK-18 (1:20) and anti-α-SMA (1:20) for 30 min at room temperature. Finally, cells were washed twice and incubated with a secondary antibody (1:500) for 30 min at room temperature. Cells were re-suspended in 1× PBS and analyzed using a BD FACSAria™ II with BD FACSDiva™ software (BD Biosciences, San Jose, CA, USA).

Cell transfection. miR-10a-5p mimics and negative control group mimics (NC mimics) were obtained from GenePharma Company (Suzhou, China). The sequences referred above are listed in Table 1. All transfections were performed with Lipofectamine 2000 reagent (Invitrogen,

Carlsbad, CA, USA) according to the manufacturer's recommendations.

RNA extraction and reverse transcription-quantitative polymerase chain reaction (RT-qPCR). Total RNA was extracted from cells using TRIzol reagent (Invitrogen, Carlsbad, CA, USA) according to the manufacturer's instructions. RNA concentration was measured using Nanodrop ZD-2000 (Applied Thermo, MA, USA). RNAs were reversed transcribed into cDNA by PrimeScript™ RT reagent Kit (TaKaRa, Otsu, Japan) in accordance with its protocol. Real-time PCR was conducted using SYBR® Premix Ex Taq™II Kit (TaKaRa, Otsu, Japan) and performed on Pikoreal 96 System (ThermoFisher Scientific, Waltham, MA, USA). The procedures of miR-10a-5p for qPCR were 95 °C for 3 min, followed by 40 cycles of 95 °C for 12 s, and 62 °C for 40 s. U6 was used as a housekeeping gene for miR-10a-5p in cells. The procedures of IL-6 and IL-8 for qPCR were 94 °C for 4 min, followed by 33 cycles of 94 °C for 1 min, 55 °C for 1 min, and 72 °C for 1 min. β-actin was used to normalize the expression levels of IL-6 and IL-8. The $2^{-\Delta\Delta ct}$ method was used to calculate the relative expression of target genes [22]. The sequences of all indicated primers are listed in Table 1. All experiments were carried out at least in triplicate.

Enzyme-linked immunosorbent assay (ELISA). The concentrations of IL-6 and IL-8 secreted from LX-2 cells, HLNFs, and HLCFs were measured by ELISA kits (R&D Systems, Minneapolis, MN, USA) according to the manufacturer's instructions by a microplate reader at a wavelength of 450 nm.

Conditioned medium (CM) preparation. The LX-2 cells transfected as previously described, HLNFs, and HLCFs were inoculated into a cell culture flask at 5×10^5 cells/flask. After 24 h, the culture medium was replaced by a serum-free medium, and the cells were placed in a cell incubator containing 5% CO_2 at 37 °C for 48 h to conduct a starvation culture. Then, the supernatant of cell culture was collected and centrifuged at 1,000 rpm for 10 min to remove dead cells. The supernatant was named CM and stored at –80 °C for subsequent experiments.

CCK-8 assay. The LX-2 cells and HLCFs transfected as previously described, as well as the SW480 cells treated with indicated CM were distributed in different wells of 96-well cell culture dish (3×10^3 cells/well). To detect cell viability, Cell Counting Kit-8 (CCK-8) (Dojindo Molecular Technologies, Shanghai, China) was added into supernatants and incubated with cells at 37 °C for 2 h and then the absorbance of cells was measured by microplate reader at 450 nm wavelength (ThermoFisher Scientific, Waltham, MA, USA). Each experiment was carried out in triplicate wells and was repeated three times.

5-ethynyl-20-deoxyuridine (EdU) incorporation assay. LX-2 cells and HLCFs transfected as previously described were distributed in different wells of 6-well cell culture plate (2×10^5 cells/well). After overnight incubation, the cells were treated by BeyoClick™ EdU-488 Proliferation Kit (Beyotime, Shanghai, China) according to the manufacturer's instructions and analyzed using a BD FACSAria™ II with BD FACSDiva™ software (BD Biosciences, San Jose, CA, USA). Each experiment was carried out in three replicate wells and was repeated three times.

Wound assay. The HLCFs transfected as previously described and the SW480 cells treated with indicated CM were plated into 6-well plates (2×10^4 cells/well) for 48 h. Then the cell monolayers were wounded with a 200 μl pipette tip to draw a gap on the plates, followed by 3 washes with 1× PBS and incubation in serum-free medium at 37 °C for 24 h and 48 h. Cells that migrated into the cleared section were observed under a microscope at specific time points. Wound closure was calculated with ImageJ software (version 1.46) (National Institutes of Health, Bethesda, MD, USA).

Transwell migration or invasion assay. A Transwell chamber culture system (Corning, Corning, NY, USA) was used to detect the migration or invasion capability of cells. 1×10^5 LX-2 cells after transfection or SW480 cells were seeded in the Transwell upper chamber without or with Matrigel-coated inserts with serum-free opti-MEM (Gibco, Carlsbad, CA, USA). A complete growth medium containing 20% FBS, 100 U/ml penicillin, and 0.1 mg/ml streptomycin was added to the lower chamber. For the invasion assay, Matrigel (BD Biosciences, San Jose, CA, USA) was thawed at 4 °C, then 50 μl Matrigel solution (matrigel : medium, 1:3) was added to the precooled inserts and solidified in a 37 °C incubator for 1 h. After incubation at 37 °C and 5% CO_2 for 24 h (migration) or 48 h (invasion), the upper side of the filter membrane was wiped with a cotton swab to remove cells. The cell inserts were fixed with 33% (v/v) acetic acid (glacial acetic acid:methyl alcohol, 1:3) for 30 min and stained with 0.1% (v/v) crystal violet (Solarbio, Beijing, China) for 20 min. Representative fields were photographed and the numbers of migrated cells

Table 1. Primer sequences.

Name	Sequence (5'→3')
miR-10a-5p mimics	F: UAC CCU GUA GAU CCG AAU UUG UG
	R: CAA AUU CGG AUC UAC AGG GUA UU
NC mimics	F: UUC UCC GAA CGU GUC ACG UTT
	R: ACG UGA CAC GUU CGG AGA ATT
miR-10a-5p	F: TGC GGT ACC CTG TAG ATC CG
	R: CCA GTG CAG GGT CCG AGG T
U6	F: ATT GGA ACG ATA CAG AGA AGA TT
	R: GGA ACG CTT CAC GAA TTT G
IL-6	F: ACT CAC CTC TTC AGA ACG AAT TG
	R: CCA TCT TTG GAA GGT TCA GGT TG
IL-8	F: TTT TGC CAA GGA GTG CTA AAG A
	R: AAC CCT CTG CAC CCA GTT TTC
β-actin	F: ACT GTG CCC ATC TAC GAG G
	R: GAA AGG GTG TAA CGC AAC TA

Abbreviations: miR-10a-5p-microRNA-10a-5p; NC-negative control; F-forward; R-reverse

per field were counted by using a light microscope (Olympus, Tokyo, Japan). Three independent experiments were repeated to get the mean value.

Cell-matrix adhesion assay. 96-well plates were coated 3 h with 2 mg/ml Matrigel at 37 °C and were blocked with 1% BSA for 2 h. The SW480 cells treated with indicated CM at 48 h were suspended in complete medium and seeded on the 96-well plates at a density of 2×10^4/well in triplicate, allowed to adhere at 37 °C for at 30 min, 60 min, or 90 min, and then were washed three times with phosphate-buffered saline. Images of adherent cells were captured using a light microscope and the quantitative results of adhered cells were determined using CCK-8 assay.

Sphere formation assay. For sphere formation, the SW480 cells treated with indicated CM at 48 h were plated on low adhesion 6-well plates (Corning, Corning, NY, USA) in a density of 3,000/well and cultured in MEM-α supplemented with 10% FBS, 100 U/ml penicillin, and 0.1 mg/ml streptomycin at 37 °C for 10 days. After observation under a microscope, representative images were captured and the number of spheroid amount per well was counted.

Statistical analysis. Statistical analysis was performed using SPSS software version 17 (SPSS Inc., Chicago, IL, USA). Each experiment was carried out in triplicate at least and all results were presented as mean ± SD. Student's t-test was used to assess statistical significance. A value of $p<0.05$ was considered significant.

Results

Overexpression miR-10a-5p inhibits LX-2 cells activation. The LX-2 cell line established by Friedman in 2005 shows the phenotype of activated hepatic stellate cells [23]. To explore whether miR-10a-5p influences the activation of LX-2 cells, miR-10a-5p mimics were transfected into the LX-2 cells to enhance the expression of miR-10a-5p. Compared with the negative control group, the expression of miR-10a-5p was enhanced by approximately 17-fold in the miR-10a-5p mimics group (***$p<0.001$, Figure 1A). Then, we detected the effects of miR-10a-5p overexpression on cell proliferative and migratory abilities of LX-2 cells. CCK-8 assay showed that overexpression of miR-10a-5p suppressed LX-2 cells viability at 2, 3, 4 days post-transfection (*$p<0.05$; *$p<0.05$; **$p<0.01$, respectively, Figure 1B). To further confirm the inhibitory effect of miR-10a-5p on LX-2 cells proliferation, an EdU assay was performed to detect proliferating cells. The results revealed a significantly lower proliferation rate of LX-2 cells following treatment with miR-10a-5p compared with the control (**$p<0.01$, Figure 1C). The Transwell migration assay indicated that overexpression of miR-10a-5p reduced the migratory ability of LX-2 cells after 24 h (***$p<0.001$, Figure 1D). In addition, the effect of miR-10a-5p on the secretion of IL-6 and IL-8 by LX-2 cells was analyzed by the ELISA assay. The results showed that LX-2 cells transfected with miR-10a-5p mimics decreased the concentration of IL-6 and IL-8 in condition medium (CM) with 20.8% and 30.1%, respectively (**$p<0.01$; *$p<0.05$, Figure 1E). RT-qPCR assay showed that miR-10a-5p overexpression also suppressed the expression of IL-6 and IL-8 in LX-2 cells (***$p<0.001$; ***$p<0.001$, Figure 1F). These results demonstrated that miR-10a-5p could inhibit the LX-2 cells activation, including proliferation, migration, and secretion abilities.

LX-2-miR-10a-5p CM suppresses SW480 cells migration, invasion, and spheroid formation. To elucidate if the activity of LX-2 cells affected malignancy of primary colorectal cancer cells, the migration, invasion, and spheroid formation abilities of SW480 cells treated with CM from LX-2-miR-10a-5p cells (LX-2 cells transfected with miR-10a-5p mimics) were analyzed. As shown in Figures 2A and 2B, there were no significant differences in cell proliferation and cell adhesion abilities between the LX-2-NC CM group and the LX-2-miR-10a-5p CM group ($p>0.05$, $p>0.05$). Whereas the invasion (Figure 2C), migration (Figure 2D), and spheroid formation (Figure 2E) abilities of SW480 cells treated with LX-2-miR-10a-5p CM were markedly decreased (***$p<0.001$, **$p<0.01$, *$p<0.05$), respectively. These results indicated that decreased cells activation caused by miR-10a-5p overexpression potentially inhibited colon cancer cells metastasis by affecting the microenvironment.

Establishment and identification of HLNFs and HLCFs. To further confirm the role of miR-10a-5p on the activation of HLCFs, the HLNFs and HLCFs isolated from a colon cancer patient with liver metastasis were established. Cells were isolated and purified by a repeated adherence method. Then, morphological characteristics were observed under a light microscope. The passaged fibroblasts from normal liver tissues exhibited a long fusiform shape in bundles or braids with consistent size, while the passaged fibroblasts from liver cancer tissues showed a flat fusiform shape with different sizes and disorder growth (Figure 3A). Immunofluorescence staining showed that cytokeratin 18 (CK-18), a well-known marker of epithelial cells, was neither expressed in HLNFs nor in HLCFs (Figure 3B). In addition, fibroblast-specific protein 1 (FSP-1), a specific marker of fibroblast expression [24], was expressed in both of the two cell lines (Figure 3C). The alpha-smooth muscle actin (α-SMA), a marker of tumor-associated fibroblasts [25], was weakly expressed in HLNFs and strongly expressed in HLCFs (Figure 3D). Next, the FACS analysis demonstrated that the positive ratios of the negative isotype, CK-18 and α-SMA were approximately 0% (Figure 3E), 0% (Figure 3F), and 95% (Figure 3G), respectively. These data indicated that these two primary cells we established, were HLNFs and HLCFs and their features and purities were qualified for further experiments.

Overexpression of miR-10a-5p inhibits HLCFs activation. Next, we compared the expression of miR-10a-5p and the secretion of IL-6 and IL-8 between HLNFs and HLCFs. The miR-10a-5p level in HLCFs was markedly lower than that in HLNFs (*$p<0.05$, Figure 4A). The concentrations of

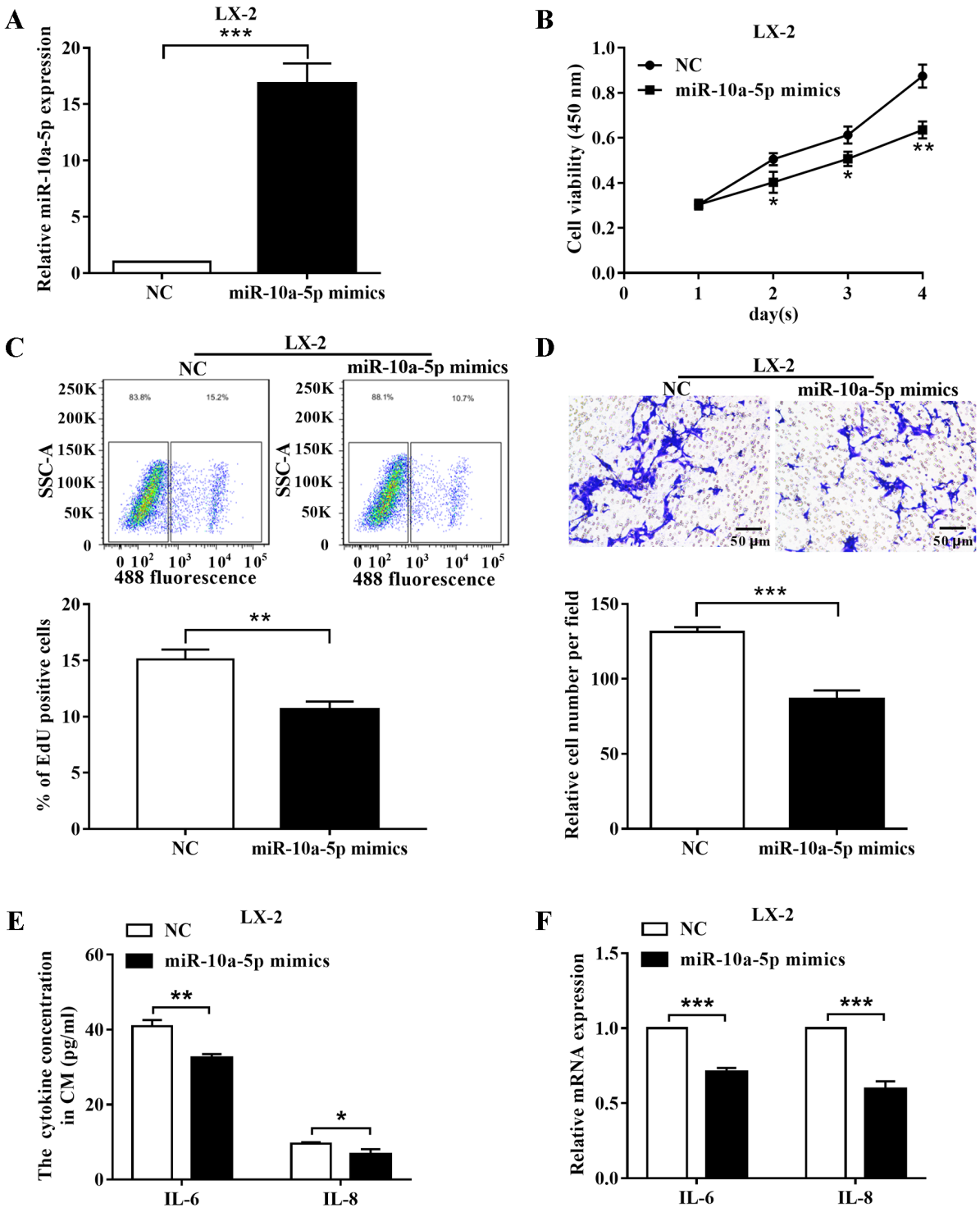

Figure 1. miR-10a-5p overexpression inhibits the LX-2 cells activation. The LX-2 cells were transfected with miR-10a-5p mimics or negative control (NC), respectively. A) The miR-10a-5p expressions in the miR-10a-5p mimics group and the NC group were detected by RT-qPCR at 24 h post-transfection. U6 was used as an internal control. B) The cell viabilities of the miR-10a-5p mimics group and the NC group were analyzed by CCK-8 assay at 1–4 day (s) post-transfection. C) The proliferation abilities of the miR-10a-5p mimics group and the NC group in LX-2 cells were detected by the EdU incorporation assays. D) The migration abilities of the miR-10a-5p mimics group and the NC group were detected by Transwell assay with Matrigel at 24 h post-transfection (magnification 200×). E) The concentrations of IL-6 and IL-8 in condition medium (CM) from LX-2 cells treated with miR-10a-5p mimics and NC for 72 h were detected by ELISA assay. F) The expression of IL-6 and IL-8 were detected in LX-2 cells treated with miR-10a-5p mimics or NC by RT-qPCR. The β-actin was used as an internal control. Each experiment was performed in triplicate (*p<0.05; **p<0.01; ***p<0.001).

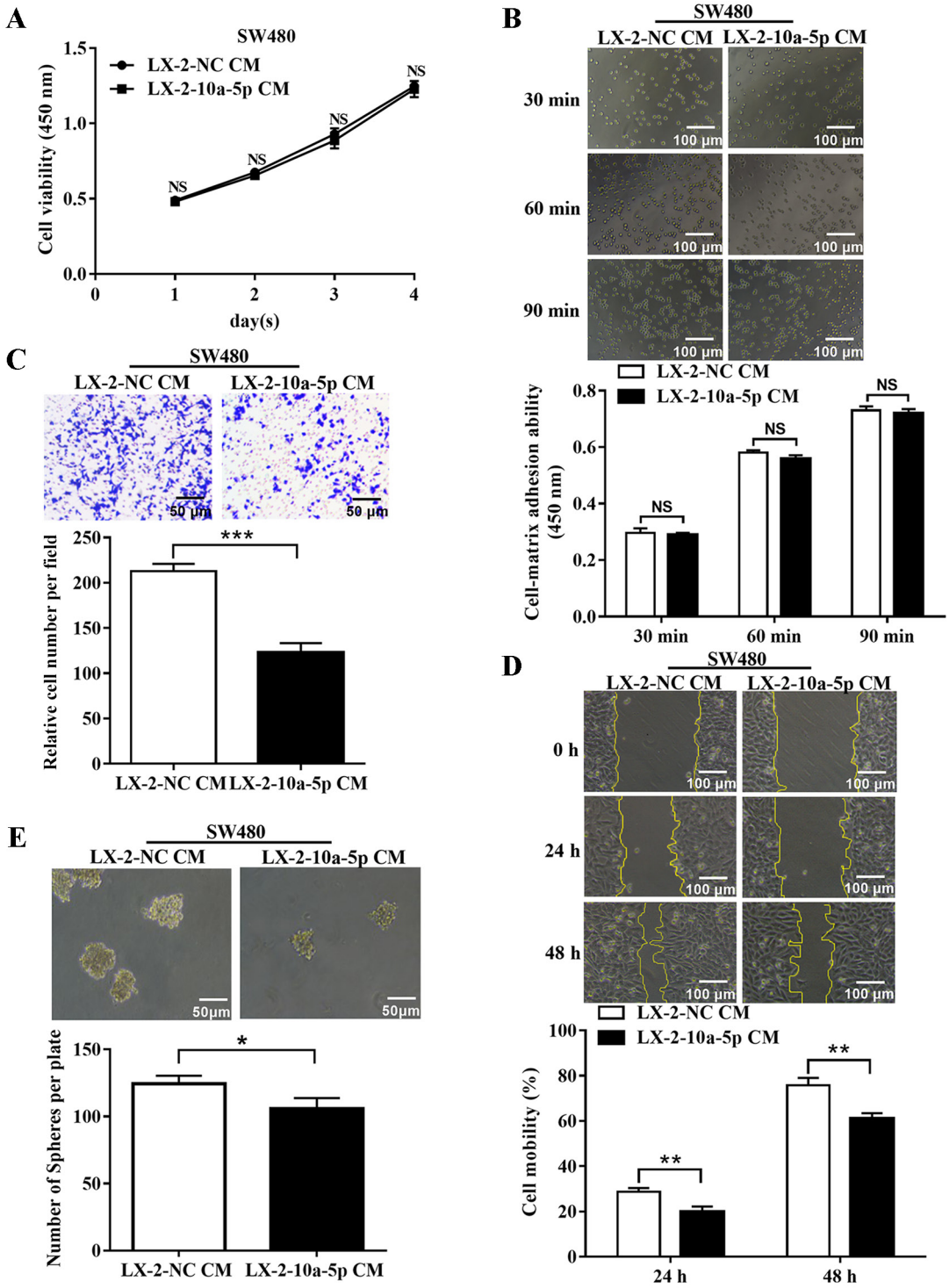

Figure 2. LX-2-miR-10a-5p CM suppresses migration, invasion, and spheroid formation abilities of SW480 cells. SW480 cells were treated with indicated CM from LX-2 cells transfected with miR-10a-5p mimics (LX-2-miR-10a-5p) or from LX-2 cells transfected with NC (LX-2-NC), respectively. A) The cell viability of SW480 cells treated as indicated was detected by CCK-8 assay. B) Cell-matrix adhesion ability of SW480 cells treated as above was detected at 30/60/90 min (magnification 100×). Quantitative results of three independent experiments (bottom). C) The cell invasion capacity of SW480 cells treated as indicated was tested by Transwell invasion assay after 48 h (magnification 200×). D) The cell migratory abilities of SW480 cells in the LX-2-miR-10a-5p CM group and the LX-2-NC CM group were analyzed by wound-healing assay (magnification 100×). E) The spheroid formation abilities of SW480 cells cultured with LX-2-miR-10a-5p CM and LX-2-NC CM for 10 days were examined by spheroid formation assay, respectively (magnification 200×). The number of cell spheroid amounts per well was analyzed (bottom). All the experiments were performed at least in triplicate (*p<0.05; **p<0.01; ***p<0.001).

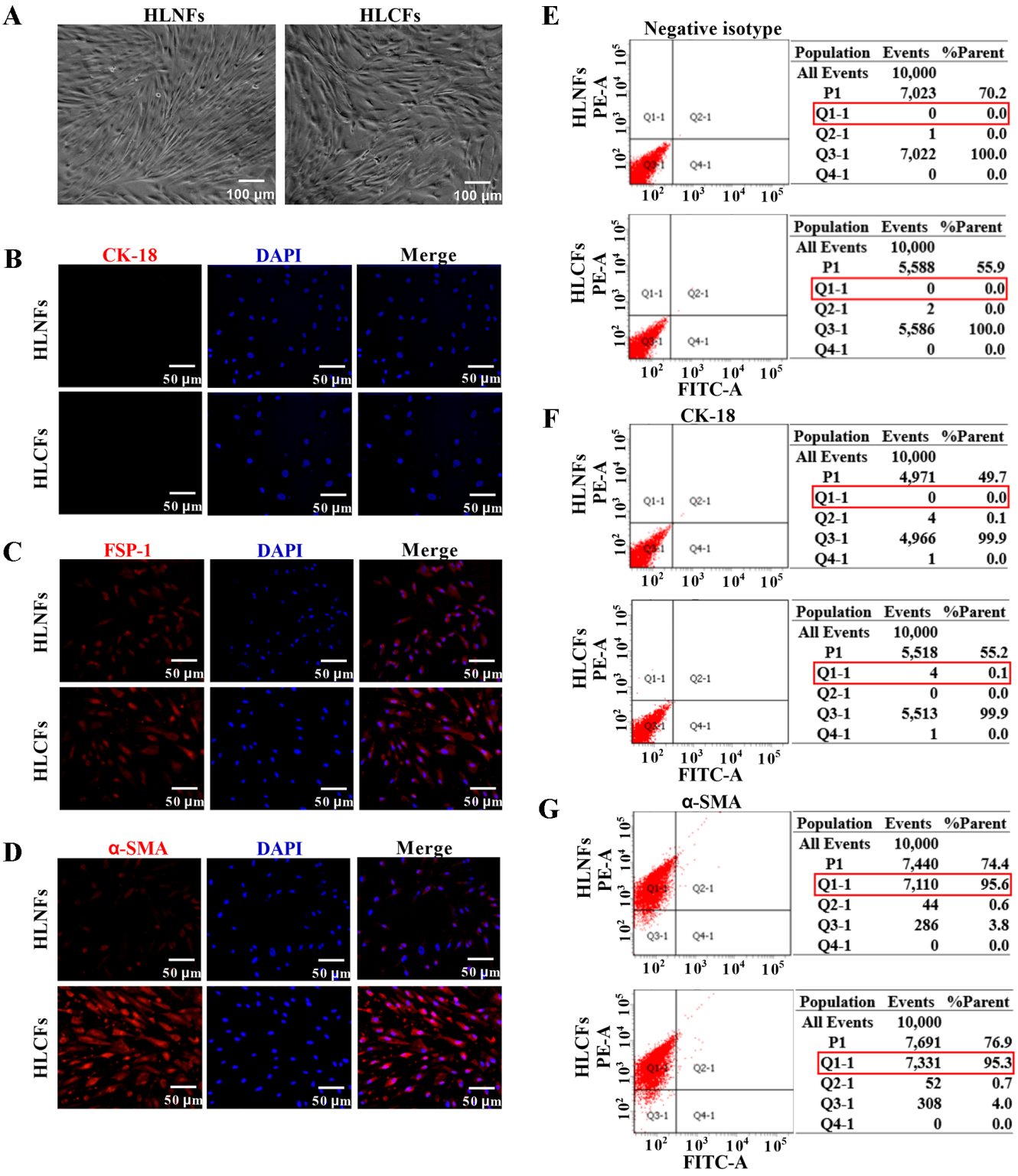

Figure 3. Establishment and identification of HLNFs and HLCFs. A) Morphological observation of human liver normal fibroblasts (HLNFs) and human liver cancer fibroblasts (HLCFs) (magnification 100×). B–D) Immunofluorescence images of NHLFs and THLFs stained with CK-18 (B), FSP-1 (C), and α-SMA (D) (red, magnification 200×). DAPI was used for nuclear staining (blue). E–G) Negative isotype (E) was a blank control. The positive rates of CK-18 (F) and α-SMA (G) in NHLFs or THLFs were analyzed by FACS assay. Each experiment was performed in triplicate.

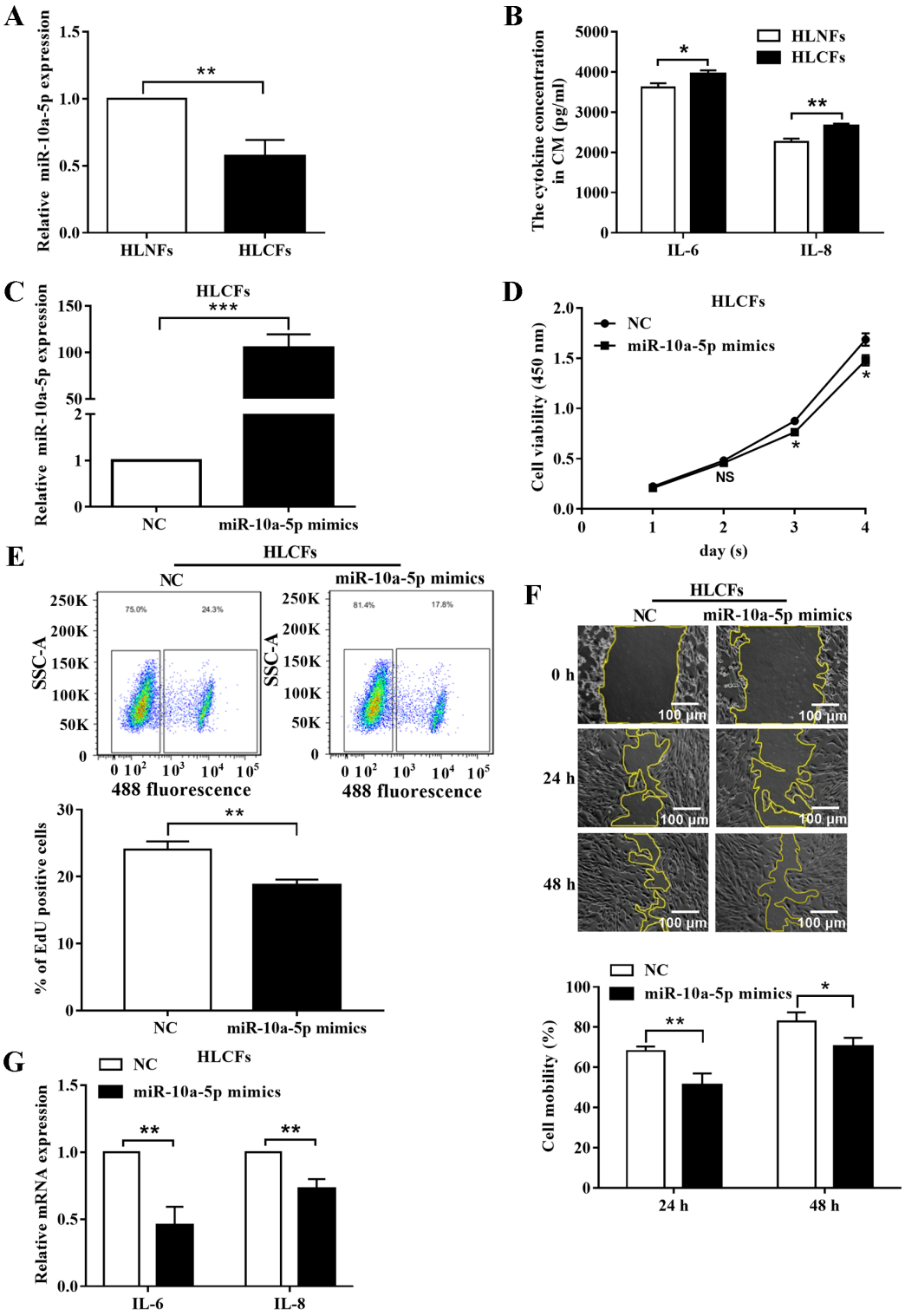

Figure 4. miR-10a-5p overexpression inhibits the HLCFs activity. A) The miR-10a-5p expression in HLNFs and HLCFs was detected by RT-qPCR. B) The concentrations of IL-6 and IL-8 in CM from the HLNFs and HLCFs were assessed by ELISA assay. C) The miR-10a-5p expression in HLCFs treated with miR-10a-5p mimics or NC was detected by RT-qPCR. D) The cell viability of HLCFs with miR-10a-5p overexpression was examined by CCK-8 assay at the indicated time. E) The proliferation ability of the miR-10a-5p mimics group and the NC group in HLCFs cells were detected by the EdU incorporation assays. F) The migration ability of HLCFs transfected with miR-10a-5p mimics or NC was estimated by wound-healing assay at 24/48 h post-transfection (magnification 100×). G) The mRNA levels of IL-6 and IL-8 in HLCFs treated with miR-10a-5p mimics or NC were tested by RT-qPCR. The β-actin was used as an internal control. Each experiment was performed in triplicate (*p<0.05; **p<0.01; ***p<0.001).

IL-6 and IL-8 in HLCFs CM were higher than HLNFs CM (*p<0.05; **p<0.01, Figure 4B). Then, HLCFs were transfected with miR-10a-5p mimics (miR-10a-5p mimics group) or negative control oligo (NC group). At 24 h post-transfection, the expression of miR-10a-5p in the miR-10a mimics group was highly increased as compared to that in the NC group (***p<0.001, Figure 4C). miR-10a-5p overexpression significantly suppressed the proliferation of HLCFs at 3- and 4-days post-transfection (p>0.05; *p<0.05; *p<0.05, Figure 4D). Consistently, EdU assay also revealed that miR-10a-5p significantly inhibited cell proliferation of HLCFs cells (**p<0.01, Figure 4E). The wound healing assay showed that migration ability of the miR-10a-5p mimics group was markedly decreased as compared to the NC group (**p<0.01; *p<0.05, Figure 4F). Both the IL-6 and IL-8 were downregulated in the miR-10a-5p mimics group compared with the NC group (**p<0.01; **p<0.01, Figure 4G). These data suggested that miR-10a-5p could inhibit the activity of HLCF cells.

HLCFs CM promotes SW480 cells migration, invasion, and spheroid formation. To confirm the results of Figure 2, the affection of HLCFs CM on invasion, migration, and spheroid formation abilities of SW480 cells was detected. There was no difference between the SW480 cells proliferation abilities treated with HLNFs CM (HLNFs group) and HLCFs CM (HLCFs group) within four days (all p>0.05, Figure 5A). The cell adhesion abilities also exhibited no alteration in the two groups at 30 min, 60 min, and 90 min (p>0.05, Figure 5B). However, SW480 cells treated with HLCFs CM exhibited stronger invasion (Figure 5C), migration (Figure 5D), and cell spheroid formation abilities (Figure 5E) that those of the HLNFs group (***p<0.001, **p<0.01, *p<0.05), respectively. In summary, deactivation of HLCFs induced by miR-10a-5p could suppress migration and invasion of colon cancer cells by affecting the microenvironment.

Discussion

In this study, we identified that the miR-10a-5p was frequently hypoexpressed in the activated liver fibroblasts. Overexpression of miR-10a-5p inhibits the proliferation and migration of LX-2 and HLCFs cells, as well as the secretion or expression level of IL-6/IL-8 in these fibroblasts, suggesting that miR-10a-5p could inhibit the activation of fibroblasts in the liver microenvironment. Consequently, the suppressed activation of fibroblasts restrained the invasion, migration, and stemness activities of SW480 cells.

It has been reported that activated fibroblasts were recognized as an abundant and active stromal cell population in the TME, and functioned as the remodeling machine to aid the creation of a desmoplastic tumor niche [26]. Emerging evidences showed that the status of the fibroblasts in the microenvironment plays an important role in cancer metastasis. For example, miR-1, miR-206, and miR-31-mediated FOXO3a/VEGF/CCL2 signaling played a prominent role in the transformation of NFs into CAFs, which promoted lung cancer cells migration, colony formation, tumor growth, and TAMs recruitment [27]. The exosomes miR-1249-5p, miR-6737-5p, and miR-6819-5p promoted human colon fibroblasts activation by inhibiting the expression of tumor protein p53 (TP53), thus accelerated tumor progression [28]. Recently, the hepatic stellate LX-2 cells differentiated into carcinoma-associated fibroblasts have been proved to facilitate liver metastasis of CC [29]. In our study, the proliferation and migration activities of LX-2 cells were both suppressed by the miR-10a-5p overexpression. In addition, the secretion of IL-6 and IL-8 of LX-2 cells was decreased. The similar phenotypic change of the HLCFs induced by miR-10a-5p overexpression revealed that miR-10a-5p could inhibit the activation of fibroblasts in the liver. Furthermore, our previous study has reported that miR-10a was hyperexpressed in the primary CRC tissues and cell lines, and miR-10a overexpression could suppress SW480 cells to metastasis to the liver by modulating epithelial-to-mesenchymal and anoikis [30]. The recent research in our lab has proved that exosomal-miR-10a from the SW480 cells can be released into the serum and cell media to inhibit the lung fibroblasts migration and IL-6/IL-8/IL-1β expression, which partly inhibit the CRC metastasis to the lung [21]. In the present study, we put forward to the reduced invasion, migration, and stemness of SW480 cells, affected by the CM from LX-2 cells and primary fibroblasts with miR-10a-5p overexpression, restricted SW480 cells metastasis to the liver. In our previous study, SW480 cells have been proved to have endogenous high expression of miR-10a and could produce exosomal-miR-10a. Hence, the role of miR-10a-5p in autonomous and non-autonomous manners could be a potential mechanism in regulation cell viability and adhesion activities of SW480 cells, which did not exhibit significant differences between the two groups induced by miR-10a-5p (Figure 2A/B). However, the specific regulatory mechanisms of SW480 cells' autonomous and non-autonomous manners of miR-10a-5p should be investigated in the future.

The massive secretion of pro-inflammatory cytokine has been recognized to be able to form an inflammatory microenvironment and promote disease development. For example, the activated fibroblasts secreted pro-inflammatory cytokines IL-6 and IL-8 to promote liver cancer progression [31]. Downregulated miR-10a could promote the production of various inflammatory cytokines by leading to activation of NF-κB signaling, including TNF-α, IL-1β, IL-6, and IL-8 in the fibroblast-like synoviocytes (FLSs), thereby promoting the proliferation, migration, and invasion of FLSs and the progression of rheumatoid arthritis [32]. In human mesangial cells (HMCs), miR-10a inhibited the IL-8 secretion by directly targeting IL-8, thereby inhibiting the proliferation of HMC cells and the progression of lupus nephritis [33]. Our results suggested that miR-10a-5p could inhibit the secretion or expression of IL-6 and IL-8 in LX-2 and HLCFs cells, which was probably an important factor in inhibiting liver metastasis of CC. As IL-8 had been identified as a direct target

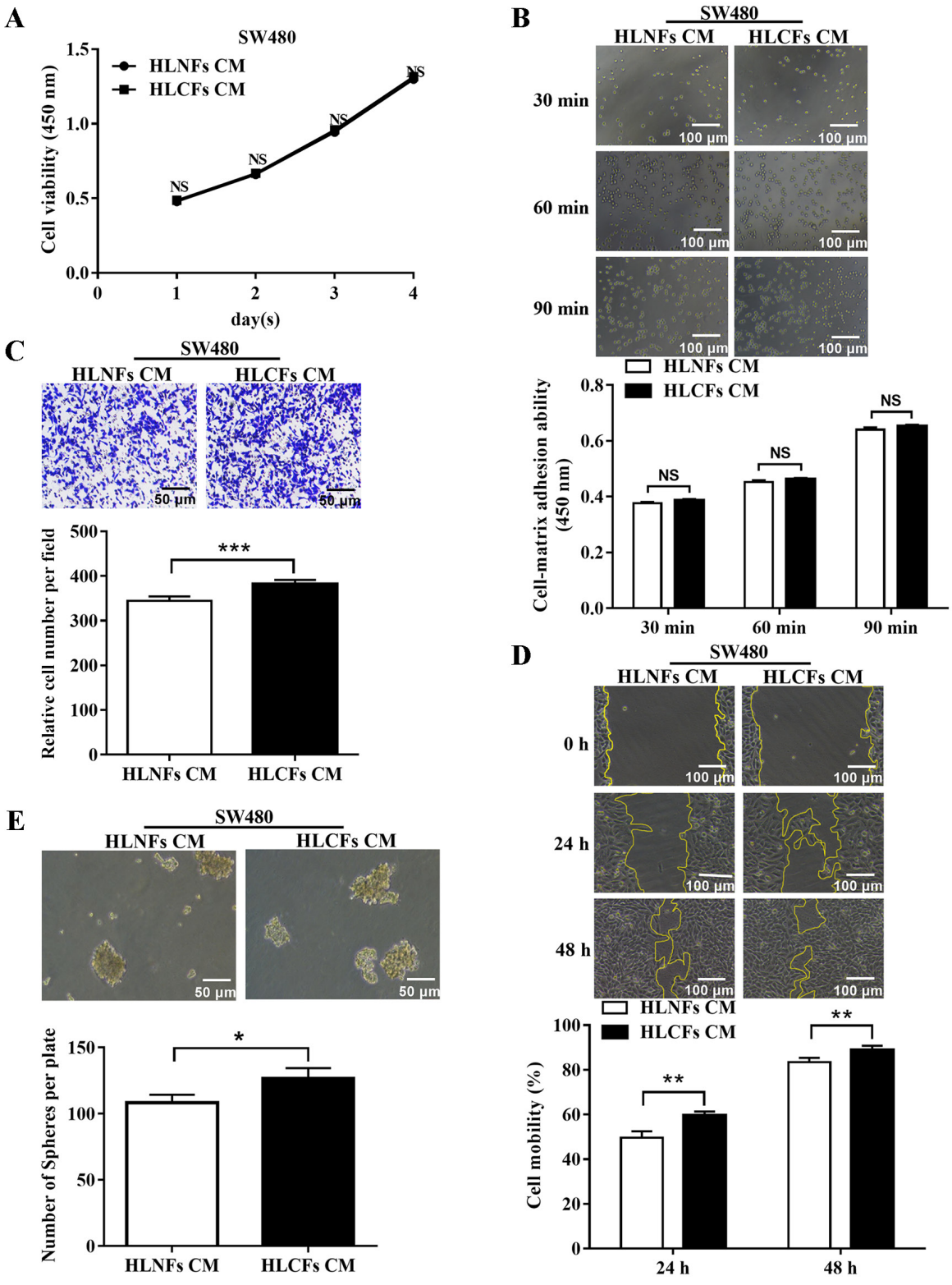

Figure 5. HLCFs CM promotes SW480 cells' migration, invasion, and stemness. SW480 cells were treated with HLNFs CM and HLCFs CM, respectively. The cell viability (A), cell-matrix adhesion activity (B), invasion capacity (C), migratory ability (D), and cell stemness (E) of the two group SW480 cells were respectively detected by CCK-8 assay, cell-matrix adhesion assay, Transwell invasion assay, wound-healing assay, spheroid formation assay. Each experiment was performed in triplicate (*p<0.05; **p<0.01, ***p<0.001).

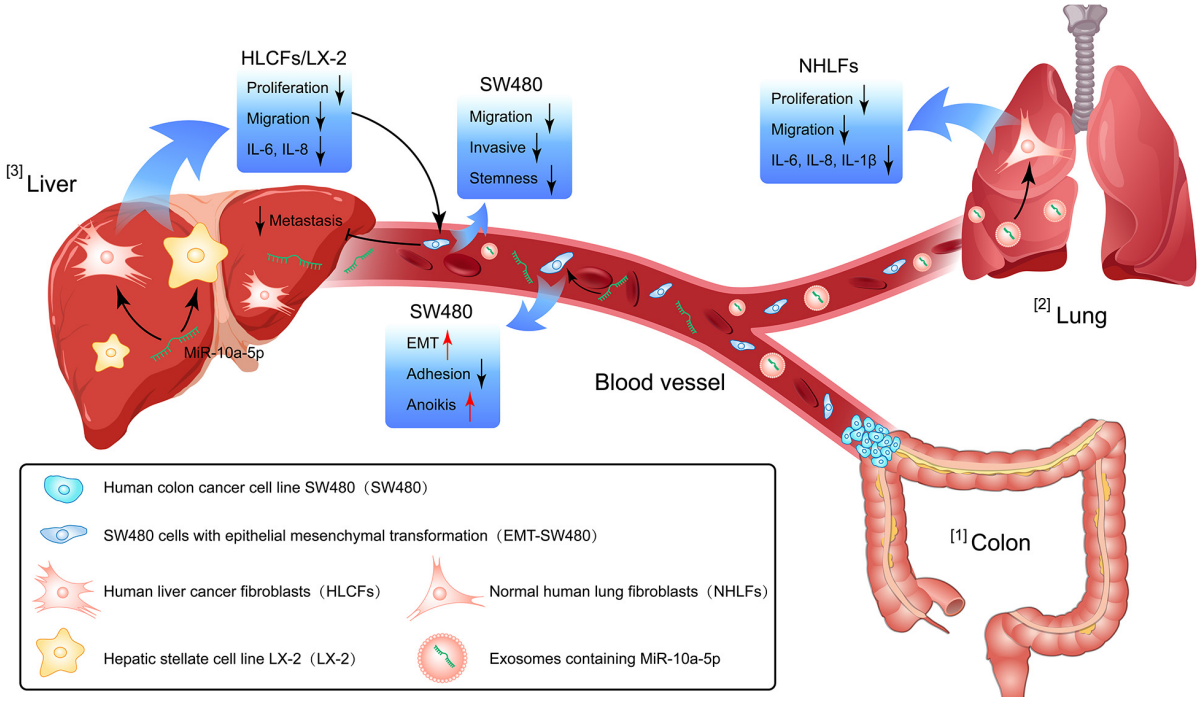

Figure 6. Proposed schematic diagram of miR-10a-5p mediating the decrease of fibroblasts activation to inhibit colon cancer metastasis. Notes: [1] = Liu et al. [30]; [2] = Wang et al. [21]; [3] = research content of this article

of miR-10a in HMCs [33], the regulation of the relationship between miR-10a-5p and IL-6 and IL-8 in human liver fibroblasts needs to be further studied.

In conclusion, our results indicate that miR-10a-5p inhibits the activation of liver fibroblasts, and the subsequently phenotypic alterations of fibroblasts suppressed SW480 cells metastasis to the liver (Figure 6). Our study on the crosstalk between the tumor cells and fibroblasts provides a new insight for liver metastases of CC, which contributes to efficient prevention and therapeutic strategies for CC.

Acknowledgments: This work was supported by the Talent Training Subsidy Project of Hebei Province (grant no. A201902029), the Natural Science Foundation of Hebei Province (grant no. H2018105049), the Science and Technology Project of Tangshan City (grant no. 19150246E), and Hebei Key Laboratory of Molecular Oncology (grant no. SZX2020043).

References

[1] CASSIDY S, SYED BA. Colorectal cancer drugs market. Nat Rev Drug Discov 2017; 16: 525–526. https://doi.org/10.1038/nrd.2017.59

[2] ZHU J, TAN Z, HOLLIS-HANSEN K, ZHANG Y, YU C et al. Epidemiological Trends in Colorectal Cancer in China: An Ecological Study. Dig Dis Sci 2017; 62: 235–243. https://doi.org/10.1007/s10620-016-4362-4

[3] ZHAO P, ZHANG Z. TNF-α promotes colon cancer cell migration and invasion by upregulating TROP-2. Oncol Lett 2018; 15: 3820–3827. https://doi.org/10.3892/ol.2018.7735

[4] CHAKEDIS J, SCHMIDT CR. Surgical Treatment of Metastatic Colorectal Cancer. Surg Oncol Clin N Am 2018; 96: e8784. https://doi.org/10.1038/nrd.2017.59

[5] PESSAUX P, CHENARD MP, BACHELLIER P, JAECK D. Consequences of chemotherapy on resection of colorectal liver metastases. J Visc Surg 2010; 147: e193–201. https://doi.org/10.1016/j.jviscsurg.2010.06.004

[6] GENG L, CHAUDHURI A, TALMON G, WISECARVER JL, ARE C et al. MicroRNA-192 suppresses liver metastasis of colon cancer. Oncogene 2014; 33: 5332–5340. https://doi.org/10.1038/onc.2013.478

[7] UROSEVIC J, GARCIA-ALBÉNIZ X, PLANET E, REAL S, CÉSPEDES MV et al. Colon cancer cells colonize the lung from established liver metastases through p38 MAPK signalling and PTHLH. Nat Cell Biol 2014; 16: 685–694. https://doi.org/10.1038/ncb2977

[8] FIDLER IJ. The pathogenesis of cancer metastasis: the 'seed and soil' hypothesis revisited. Nature reviews. Cancer 2003; 3: 453–458. https://doi.org/10.1038/nrc1098

[9] JOYCE J A, POLLARD JW. Microenvironmental regulation of metastasis. Nat Rev Cancer 2009; 9: 239–252. https://doi.org/10.1038/nrc2618

[10] ZHANG Q, PENG C. Cancer-associated fibroblasts regulate the biological behavior of cancer cells and stroma in gastric cancer. Oncol Lett 2018; 15: 691–698. https://doi.org/10.3892/ol.2017.7385

[11] KALLURI R, ZEISBERG M. Fibroblasts in cancer. Nat Rev Cancer 2006; 6: 392–401. https://doi.org/10.1038/nrc1877
[12] LIAO Z, TAN ZW, ZHU P, TAN NS. Cancer-associated fibroblasts in tumor microenvironment - Accomplices in tumor malignancy. Cell Immunol 2019; 343: 103729. https://doi.org/10.1016/j.cellimm.2017.12.003
[13] KOJIMA Y, ACAR A, EATON E N, MELLODY K T, SCHEEL C et al. Autocrine TGF-beta and stromal cell-derived factor-1 (SDF-1) signaling drives the evolution of tumor-promoting mammary stromal myofibroblasts. Proc Natl Acad Sci U S A 2010; 107: 20009–20014. https://doi.org/10.1073/pnas.1013805107
[14] TANG X, HOU Y, YANG G, WANG X, TANG S et al. Stromal miR-200s contribute to breast cancer cell invasion through CAF activation and ECM remodeling. Cell Death Differ 2016; 23: 132–145. https://doi.org/10.1038/cdd.2015.78
[15] AMBROS V. microRNAs: tiny regulators with great potential. Cell 2001; 107: 823–826. https://doi.org/10.1016/s0092-8674(01)00616-x
[16] CHENG AM, BYROM MW, SHELTON J, FORD LP. Antisense inhibition of human miRNAs and indications for an involvement of miRNA in cell growth and apoptosis. Nucleic Acids Res 2005; 33: 1290–1297. https://doi.org/10.1038/nrc1997
[17] CALIN GA, CROCE CM. MicroRNA signatures in human cancers. Nat Rev Cancer 2006; 6: 857–866. https://doi.org/10.1093/nar/gki200
[18] TAN G, TANG X, TANG F. The role of microRNAs in nasopharyngeal carcinoma. Tumour Biol 2015; 36: 69–79. https://doi.org/10.1007/s13277-014-2847-3
[19] YANG TS, YANG XH, CHEN X, WANG XD, HUA J et al. MicroRNA-106b in cancer-associated fibroblasts from gastric cancer promotes cell migration and invasion by targeting PTEN. FEBS Lett 2014; 588: 2162–2169. https://doi.org/10.1016/j.febslet.2014.04.050
[20] LI J, GUAN J, LONG X, WANG Y, XIANG X. mir-1-mediated paracrine effect of cancer-associated fibroblasts on lung cancer cell proliferation and chemoresistance. Oncol Rep 2016; 35: 3523–3531. https://doi.org/10.3892/or.2016.4714
[21] WANG J, LIU Y, LI Y, ZHENG X, GAN J et al. Exosomal-miR-10a derived from colorectal cancer cells suppresses migration of human lung fibroblasts, and expression of IL-6, IL-8 and IL-1β. Mol Med Rep 2021; 23: 84. https://doi.org/10.3892/mmr.2020.11723
[22] LIVAK KJ, SCHMITTGEN TD. Analysis of relative gene expression data using real-time quantitative PCR and the 2(-Delta Delta C(T)) Method. Methods 2001; 25: 402–408. https://doi.org/10.1006/meth.2001.1262
[23] XU L, HUI AY, ALBANIS E, ARTHUR MJ, O'BYRNE SM et al. Human hepatic stellate cell lines, LX-1 and LX-2: new tools for analysis of hepatic fibrosis. Gut 2005; 54: 142–151. https://doi.org/10.1136/gut.2004.042127
[24] STRUTZ F, OKADA H, LO CW, DANOFF T, CARONE RL et al. Identification and characterization of a fibroblast marker: FSP1. J Cell Biol 1995; 130: 393–405. https://doi.org/10.1083/jcb.130.2.393
[25] XIONG G, HUANG H, FENG M, YANG G, ZHENG S et al. MiR-10a-5p targets TFAP2C to promote gemcitabine resistance in pancreatic ductal adenocarcinoma. J Exp Clin Cancer Res 2018; 37: 76. https://doi.org/10.1186/s13046-018-0739-x
[26] LIU T, ZHOU L, LI D, ANDL T, ZHANG Y. Cancer-Associated Fibroblasts Build and Secure the Tumor Microenvironment. Front Cell Dev Biol 2019; 7: 60. https://doi.org/10.3389/fcell.2019.00060
[27] SHEN H, YU X, YANG F, ZHANG Z, SHEN J et al. Reprogramming of Normal Fibroblasts into Cancer-Associated Fibroblasts by miRNAs-Mediated CCL2/VEGFA Signaling. PLoS Genet 2016; 12: e1006244. https://doi.org/10.1371/journal.pgen.1006244
[28] YOSHII S, HAYASHI Y, IIJIMA H, INOUE T, KIMURA K et al. Exosomal microRNAs derived from colon cancer cells promote tumor progression by suppressing fibroblast TP53 expression. Cancer Sci 2019; 110: 2396–2407. https://doi.org/10.1111/cas.14084
[29] TAN HX, GONG WZ, ZHOU K, XIAO ZG, HOU FT et al. CXCR4/TGF-β1 mediated hepatic stellate cells differentiation into carcinoma-associated fibroblasts and promoted liver metastasis of colon cancer. Cancer Biol Ther 2020; 21: 258–268. https://doi.org/10.1080/15384047.2019.1685157
[30] LIU Y, ZHANG Y, WU H, LI Y, ZHANG Y et al. miR-10a suppresses colorectal cancer metastasis by modulating the epithelial-to-mesenchymal transition and anoikis. Cell Death Dis 2017; 8: e2739. https://doi.org/10.1038/cddis.2017.61
[31] FANG T, LV H, LV G, LI T, WANG C et al. Tumor-derived exosomal miR-1247-3p induces cancer-associated fibroblast activation to foster lung metastasis of liver cancer. Nat Commun 2018; 9: 191. https://doi.org/10.1038/s41467-017-02583-0
[32] MU N, GU J, HUANG T, ZHANG C, SHU Z et al. A novel NF-κB/YY1/microRNA-10a regulatory circuit in fibroblast-like synoviocytes regulates inflammation in rheumatoid arthritis. Sci Rep 2016; 6: 20059. https://doi.org/10.1038/srep20059
[33] TANGTANATAKUL P, THAMMASATE B, JACQUET A, REANTRAGOON R, PISITKUN T et al. Transcriptomic profiling in human mesangial cells using patient-derived lupus autoantibodies identified miR-10a as a potential regulator of IL8. Sci Rep 2017; 7: 14517. https://doi.org/10.1038/s41598-017-15160-8